A Lassa Virus Live-Attenuated Vaccine Candidate Based on Rearrangement of the Intergenic Region

Yingyun Cai,[a] Masaharu Iwasaki,[b,c] Daisuke Motooka,[d] David X. Liu,[a] Shuiqing Yu,[a] Kurt Cooper,[a] Randy Hart,[a] Ricky Adams,[a] Tracey Burdette,[a] Elena N. Postnikova,[a] Jonathan Kurtz,[a] Marisa St. Claire,[a] Chengjin Ye,[e] Jens H. Kuhn,[a] Luis Martínez-Sobrido,[e] Juan Carlos de la Torre[b]

aIntegrated Research Facility at Fort Detrick, National Institute of Allergy and Infectious Diseases, National Institutes of Health, Frederick, Maryland, USA
bDepartment of Immunology and Microbiology, The Scripps Research Institute, La Jolla, California, USA
cLaboratory of Emerging Viral Diseases, International Research Center for Infectious Diseases, Research Institute for Microbial Diseases, Osaka University, Osaka, Japan
dLaboratory of Pathogen Detection and Identification, International Research Center for Infectious Diseases, Research Institute for Microbial Diseases, Osaka University, Osaka, Japan
eDepartment of Microbiology and Immunology, University of Rochester, Rochester, New York, USA

Yingyun Cai and Masaharu Iwasaki contributed equally to this article. Author order was determined on the basis of each individual's contribution to development and analysis of the work.

ABSTRACT Lassa virus (LASV) poses a significant public health problem within the regions of Lassa fever endemicity in Western Africa. LASV infects several hundred thousand individuals yearly, and a considerable number of Lassa fever cases are associated with high morbidity and lethality. No approved LASV vaccine is available, and current therapy is limited to an off-label usage of ribavirin that is only partially effective and associated with significant side effects. The impact of Lassa fever on human health, together with the limited existing countermeasures, highlights the importance of developing effective vaccines against LASV. Here, we present the development and characterization of a recombinant LASV (rLASV) vaccine candidate [rLASV(IGR/S-S)], which is based on the presence of the noncoding intergenic region (IGR) of the small (S) genome segment (S-IGR) in both large (L) and S LASV segments. In cultured cells, rLASV(IGR/S-S) was modestly less fit than wild-type rLASV (rLASV-WT). rLASV(IGR/S-S) was highly attenuated in guinea pigs, and a single subcutaneous low dose of the virus completely protected against otherwise lethal infection with LASV-WT. Moreover, rLASV(IGR/S-S) was genetically stable during serial passages in cultured cells. These findings indicate that rLASV(IGR/S-S) can be developed into a LASV live-attenuated vaccine (LAV) that has the same antigenic composition as LASV-WT and a well-defined mechanism of attenuation that overcomes concerns about increased virulence that could be caused by genetic changes in the LAV during multiple rounds of multiplication.

IMPORTANCE Lassa virus (LASV), the causative agent of Lassa fever, infects several hundred thousand people in Western Africa, resulting in many lethal Lassa fever cases. No U.S. Food and Drug Administration-licensed countermeasures are available to prevent or treat LASV infection. We describe the generation of a novel LASV live-attenuated vaccine candidate rLASV(IGR/S-S), which is based on the replacement of the large genomic segment noncoding intergenic region (IGR) with that of the small genome segment. rLASV(IGR/S-S) is less fit in cell culture than wild-type virus and does not cause clinical signs in inoculated guinea pigs. Importantly, rLASV(IGR/S-S) protects immunized guinea pigs against an otherwise lethal exposure to LASV.

KEYWORDS *Arenaviridae*, arenavirid, arenavirus, *Bunyavirales*, bunyavirus, guinea pig, Lassa, Lassa fever, Lassa virus, LASV, LAV, live-attenuated vaccine, mammarenavirus,

strain 13, vaccine, VHF, viral hemorrhagic fever, intergenic region, IGR, reverse genetics

Lassa fever (LF) was first described in Lassa, Nigeria, in 1969 (1). The causative agent of LF, Lassa virus (LASV), was subsequently discovered and isolated from LF patients and its natural host reservoir, the Natal mastomys (*Mastomys natalensis*) (2, 3). LF poses a significant public health burden in the areas where it is endemic, mainly sub-Saharan Western Africa (e.g., Guinea, Liberia, Nigeria, and Sierra Leone). A single longitudinal study conducted more than 30 years ago in Sierra Leone estimated that hundreds of thousands of LASV infections occurred annually (4). Among the people infected, 80% are asymptomatic, whereas the other 20% develop disease that usually requires hospital admission. Nevertheless, LASV infection was largely ignored as a public health threat for extended periods of time (5), and the true incidence of LASV infections and the public health burden of LF in Western Africa remain unknown but are likely significant. Case fatality rates (CFRs) of 15% to 20% have been reported among hospitalized LF patients (6). Recently, the occurrence of a high number of LF cases associated with high (up to 60%) case fatality rates in Nigeria (6, 7) triggered reevaluation of LF risk for global health security (8). Moreover, LASV expansion outside its traditional areas of endemicity and increased travel have resulted in exportation of LF cases from Western African countries where the disease is endemic to countries where it is nonendemic (9). To date, no U.S. Food and Drug Administration (FDA)-licensed countermeasures are available to prevent or treat LASV, and current anti-LASV therapy is limited to the use of ribavirin, which is only partially effective and can cause significant side effects (10, 11). Due to the impact of LF on human health and limited existing countermeasures to combat LF, the World Health Organization (WHO) included LF on the revised list of priority diseases for development of effective vaccines (12).

Like other mammarenaviruses (*Bunyavirales*: *Arenaviridae*), LASV is an enveloped virus with a bisegmented, single-stranded RNA genome (13, 14). Each viral genome segment uses an ambisense coding strategy to direct the synthesis of two viral proteins from open reading frames separated by noncoding intergenic regions (IGRs) (14). The large (L) segment encodes the large (L) protein that functions as a viral RNA (vRNA)-directed RNA polymerase and RING finger protein Z, which functions as a matrix-like protein for virion assembly and budding (15–18). The small (S) segment encodes the nucleoprotein (NP) and the glycoprotein (GP) precursor (GPC) (19–21). NP and L, together with the vRNA, form the viral L and S ribonucleoprotein complexes (vRNPs) responsible for directing replication and transcription of the viral RNA genome. NP is also involved in counteracting innate immune responses during viral infection (22–25). GPC is cotranslationally processed by cellular signal peptidase to generate a stable signal peptide (SSP) and a GPC precursor that is posttranslationally cleaved by the cellular proprotein convertase and subtilisin kexin isozyme-1/site-1 protease (SKI-1/S1P) to generate GP1 and GP2 subunits. The GP1 and GP2 subunits, together with the SSP, form mature GP peplomers on the surface of the virion envelope that mediate virion cell entry via receptor-mediated endocytosis (26–28).

For a given mammarenavirus, S-IGRs and L-IGRs differ in both sequence and predicted secondary structures. The IGRs play critical roles in mammarenavirus transcriptional control and production of infectious particles (29). The L-IGR and S-IGR of lymphocytic choriomeningitis virus (LCMV) have distinct functional roles in posttranscriptional control of viral gene expression (30, 31). The importance of the IGRs in viral multiplication has also been documented for other arenaviruses. For instance, replication of a recombinant Lujo virus with a 36-nucleotide deletion in the L-IGR was impaired in cultured cells compared to its parental virus (32). A Machupo virus with a 35-nucleotide deletion within the L-IGR was only moderately less fit in cell culture than the wild-type (WT) virus but highly attenuated *in vivo* (33).

Importantly, a recombinant LCMV containing the S-IGR in both the S and L genome segments [rLCMV(IGR/S-S)] was only modestly less fit in cultured cells than rLCMV-WT.

However, rLCMV(IGR/S-S) was highly attenuated in a laboratory mouse model of LCMV infection, but mice immunized with rLCMV(IGR/S-S) were fully protected against an otherwise lethal infection with rLCMV-WT (30).

On the basis of these promising results, we examined whether reorganization of IGRs could represent a general molecular strategy for mammarenavirus attenuation that could be applied to LASV. In line with prospective epidemiological studies in Western Africa, live-attenuated vaccines (LAVs) represent the most feasible approach to control LF, as LAVs induce long-term robust cell-mediated responses following single immunizations (34). Here, we report the generation of a recombinant LASV that contains the LASV S-IGR in both the S and L genome segments, rLASV(IGR/S-S). *In vitro*, the viral fitness of rLASV(IGR/S-S) was moderately decreased compared to rLASV-WT. *In vivo*, rLASV(IGR/S-S) was fully attenuated in both strain 13 and Hartley guinea pigs but provided full protection, upon a single subcutaneous (s.c.) low-dose administration, against an otherwise lethal exposure to LASV-WT. Our data support further development of this strategy as a general mechanism for the development of LAVs to combat human mammarenavirus infections.

RESULTS

Generation of rLASV(IGR/S-S). LASV L- and S-IGRs are different in both sequence and predicted structure (Fig. 1A). A previously established LASV mouse RNA polymerase I promoter-based reverse genetic system was used to generate a recombinant LASV containing the S-IGR in both L and S segments [rLASV(IGR/S-S)] (Fig. 1B) (35, 36). However, several attempts to rescue rLASV(IGR/S-S) were unsuccessful. As an alternative approach, we used a LASV reverse genetic system in which intracellular synthesis of L and S segment vRNAs was under the control of the Escherichia phage T7 RNA polymerase promoter (Fig. 1C). HEK293T/17 cells were transfected with the indicated set of five plasmids (Fig. 1C). On day 6 posttransfection (p.t.), tissue culture supernatants (TCS) (P0D6) were collected, and transfected HEK293T/17 cells were cocultured with fresh Vero cells. After days 10 (day 4 of coculture [P0D10]), 13 (day 7 of coculture [P0D13]), and 17 (day 11 of coculture [P0D17]) p.t., TCS were collected, and viral titers in TCS were determined for all four time points by plaque assay (Fig. 1D). At day 6 p.t., unlike rLASV-WT, infectious rLASV(IGR/S-S) was not detected in TCS. However, in cocultures of transfected HEK293T/17 with Vero cells, rLASV(IGR/S-S) was recovered at a low titer (1.5×10^3 PFU/ml) followed by an increased titer seen after transfer to fresh Vero cells (4.83×10^4 PFU/ml at P0D13) (Fig. 1D).

Characterization of rLASV(IGR/S-S). rLASV-WT and rLASV(IGR/S-S) growth kinetics were compared by inoculating interferon (IFN)-competent (A549) and IFN-deficient (Vero) cells with these viruses at different multiplicities of infection (MOIs) (Fig. 2). Viral titers were measured daily for 4 days postexposure (p.e.). rLASV(IGR/S-S) replicated efficiently in both cell types, although viral peak titers in both cell lines were up to 2 orders of magnitude lower than those of rLASV-WT (Fig. 2A and B). The plaque sizes produced by rLASV(IGR/S-S) (0.60 ± 0.21 mm in diameter) were significantly smaller than those caused by rLASV-WT (2.12 ± 0.74 mm; $n = 25$, $P < 0.0001$) (Fig. 2C). Viral spread was analyzed by immunofluorescence assay in A549 and Vero cells infected with rLASV-WT or rLASV(IGR/S-S). Both GP-positive and NP-positive cell numbers were lower in rLASV(IGR/S-S)-infected cells than in rLASV-WT-infected cells at 48 h and 72 h p.e. (Fig. 2D and E; see also Fig. S1 in the supplemental material). Reduced GP and NP expression was also observed in rLASV(IGR/S-S)-infected A549 cells by Western blotting (Fig. 2F). Taking the results together, the reorganization of IGR in LASV genome modestly reduced fitness in cultured cells.

Attenuation of rLASV(IGR/S-S) in strain 13 guinea pigs. Next, we examined whether replacement of L-IGR with S-IGR in the L segment would have an appreciable impact on LASV virulence *in vivo*. Since strain 13 guinea pigs are highly sensitive to LASV infection, with 100% lethality following s.c. exposure to 10^3 PFU (37), the safety profile of rLASV(IGR/S-S) was evaluated in strain 13 guinea pigs.
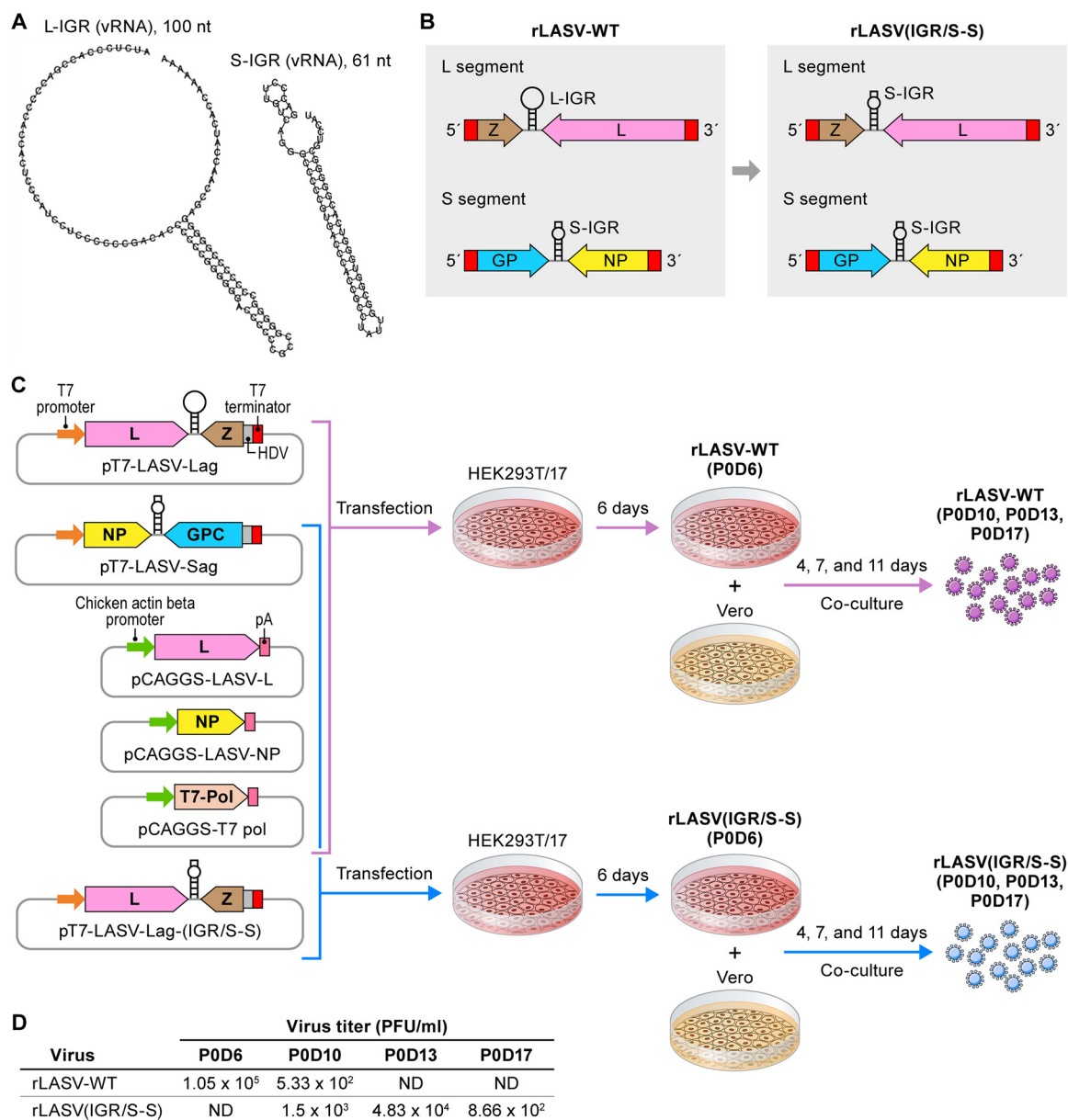
FIG 1 Generation of rLASV(IGR/S-S). (A) Comparison of LASV L-IGR and S_IGR predicted structures. Secondary structures of genomic (vRNA) L-IGR and S-IGR were determined using the RNAfold WebServer (http://rna.tbi.univie.ac.at/cgi-bin/RNAWebSuite/RNAfold.cgi). nt, nucleotide. (B) Diagram of generation rLASV(IGR/S-S). (C) Strategy for rescuing rLASV(IGR/S-S) or rLASV-WT. pT7-LASV-Sag directs the synthesis of the LASV S segment RNAs, and pT7-LASV-Lag or pT7-LASV-Lag-(IGR/S-S) directs synthesis of the LASV segment RNAs (antigenome polarity) under the control of an Escherichia phage T7 DNA-directed RNA polymerase promoter. Support plasmids pCAGGS-LASV-L and pCAGGS-LASV-NP express LASV L and NP, respectively. pCAGGS-T7 pol expresses T7 RNA polymerase. pT7-LASV-Lag-(IGR/S-S) was used instead of pT7-LASV-Lag to rescue rLASV(IGR/S-S). HEK293T/17 cells were transiently cotransfected with the indicated plasmids. At day 6 p.t., TCS were collected and transfected cells were detached and cocultured (1:1) with fresh Vero cells. TCS were harvested on p.t. day 10 (P0D10), day 13 (P0D13), and day 17 (P0D17). (D) Virus titers of rLASV-WT and rLASV(IGR/S-S) in TCS at indicated days. L-IGR, intergenic region of L segment; S-IGR, intergenic region of S segment; IGR(S-S), noncoding intergenic region (IGR) of the S genome segment (IGR-S) in both the LASV L and S segments; HDV, hepatitis delta virus ribozyme (HDV-Rbz) sequence; pA, poly(A) tail; ND, not detected.

Strain 13 guinea pigs were inoculated s.c. with 10^5 PFU of rLASV(IGR/S-S) ($n = 5$), rLASV-WT ($n = 4$), or LASV ($n = 5$). All animals inoculated with rLASV(IGR/S-S) survived to the end of the study (day 42 p.e.) (Fig. 3A) without developing any overt clinical signs of disease (Fig. 3B), including weight loss (Fig. 3C) or elevated temperature (Fig. 3D). In contrast, all animals inoculated with rLASV-WT or LASV developed several clinical signs of infection (e.g., ruffled coat, labored respiration), body weight loss, and transient
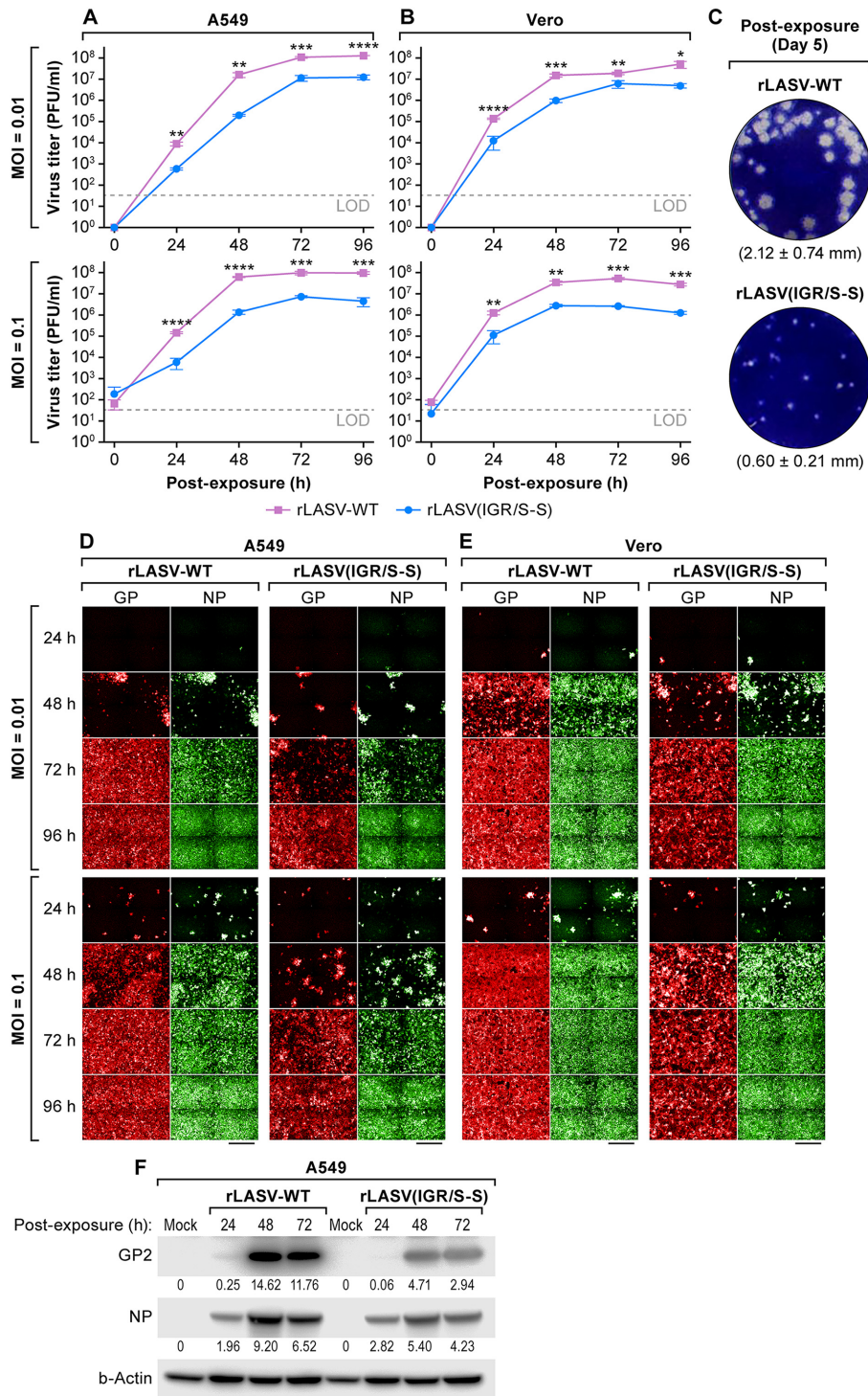
FIG 2 Growth kinetics of rLASV(IGR/S-S) in cultured cells. (A and B) A549 (A) and Vero (B) cells were inoculated with rLASV-WT or rLASV(IGR/S-S) at the indicated MOIs, and viral titers in TCS were determined by plaque assay at the indicated time points. Data represent means ± standard deviations (SD) of results from triplicate samples. Dotted lines indicate the lower limit of detection (33 PFU/ml). *, $P < 0.05$; **, $P < 0.01$; ***, $P < 0.001$; ****, $P < 0.0001$ (Student's t test). (C) Plaque morphologies and sizes of rLASV-WT (top) and rLASV(IGR/S-S) (bottom) on Vero cell monolayers. Data presented are means ± SD of measurements of 25 randomly selected plaques. (D and E) Replicates of A549 (D) and Vero (E) cells infected as described above were evaluated for LASV NP and GP expression by immunofluorescence assay using anti-LASV GP and NP monoclonal antibodies (MAbs), respectively. Representative images of three independent infection experiments are illustrated. Scale bars = 200 μm. (F) Western blot analysis of LASV-GP and NP expression in A549 cells infected with rLASV-WT or rLASV(IGR/S-S) (MOI = 0.1). Numbers below bands correspond to densitometry quantification of each band normalized to actin beta control.
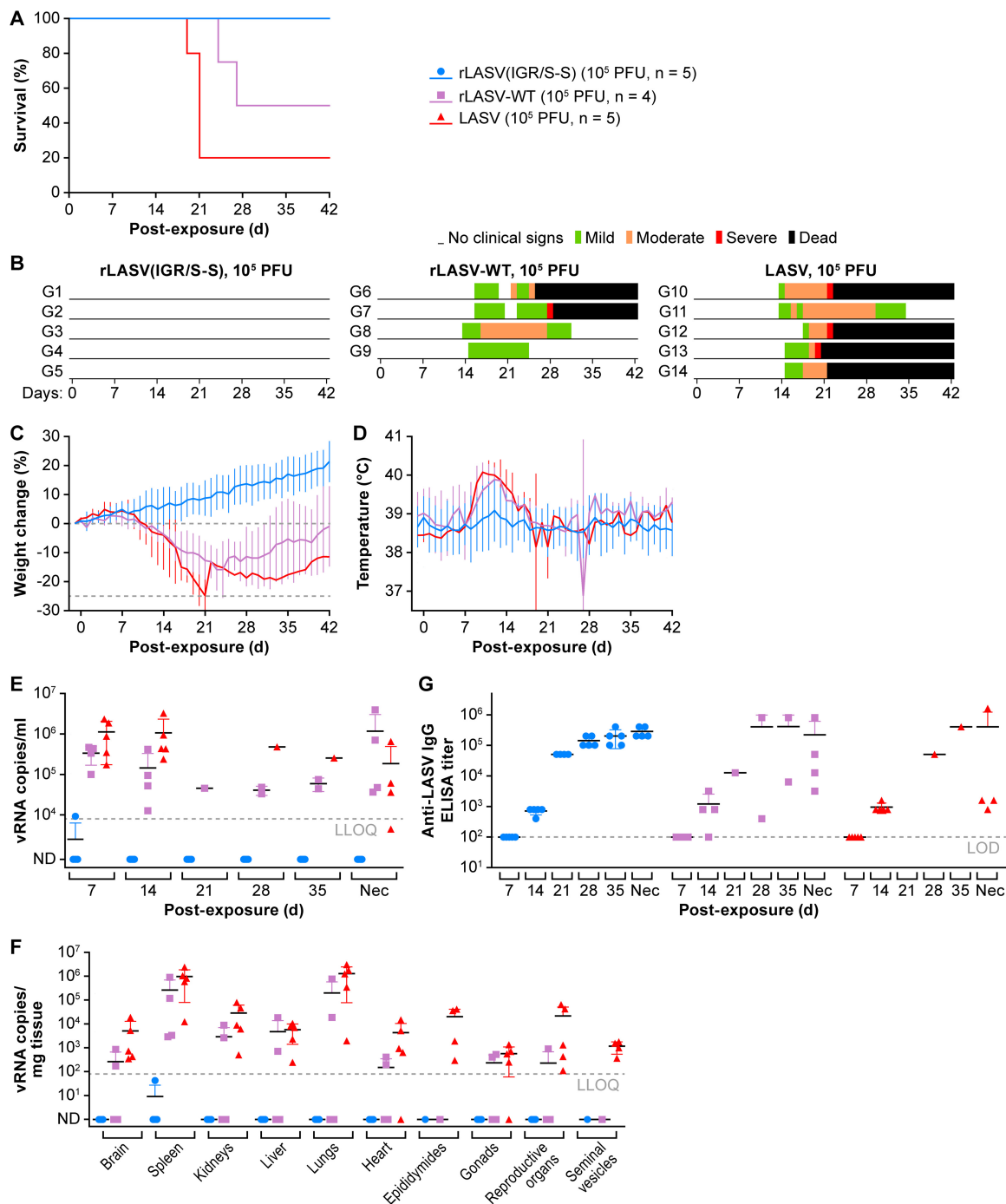
FIG 3 rLASV(IGR/S-S) is attenuated in strain 13 guinea pigs. Strain 13 guinea pigs were s.c. exposed to 10^5 PFU of rLASV(IGR/S-S) ($n = 5$, blue), rLASV-WT ($n = 4$, purple), or LASV ($n = 5$, red). (A to D) Survival (A), clinical scores (B), body weight loss (C), and temperature changes (D) were monitored daily for 42 days. (E and F) Viral loads in the blood at different times p.e. (E) and viral loads in the indicated tissues at necropsy (F) were measured by RT-qPCR. (G) Anti-LASV IgG plasma titers were determined by ELISA at the indicated days p.e. LLOQ, lower limit of quantification (panels E and F); LOD, limit of detection (panel G); ND, not detected; Nec, necropsy date; d, day.

elevated temperatures (Fig. 3B, C, and D, respectively). Two of 4 rLASV-WT-exposed and 4 of 5 LASV-exposed guinea pigs eventually met euthanasia criteria. Viral loads in blood at the different times p.e. (Fig. 3E) and in the indicated tissues at the end of the study (Fig. 3F) were measured by reverse transcription-quantitative PCR (RT-qPCR). vRNAs were not detected in the blood collected at days 7, 14, 21, 28, 35, and 42 p.e. from the majority of rLASV(IGR/S-S)-inoculated guinea pigs. Low concentrations of viral RNA
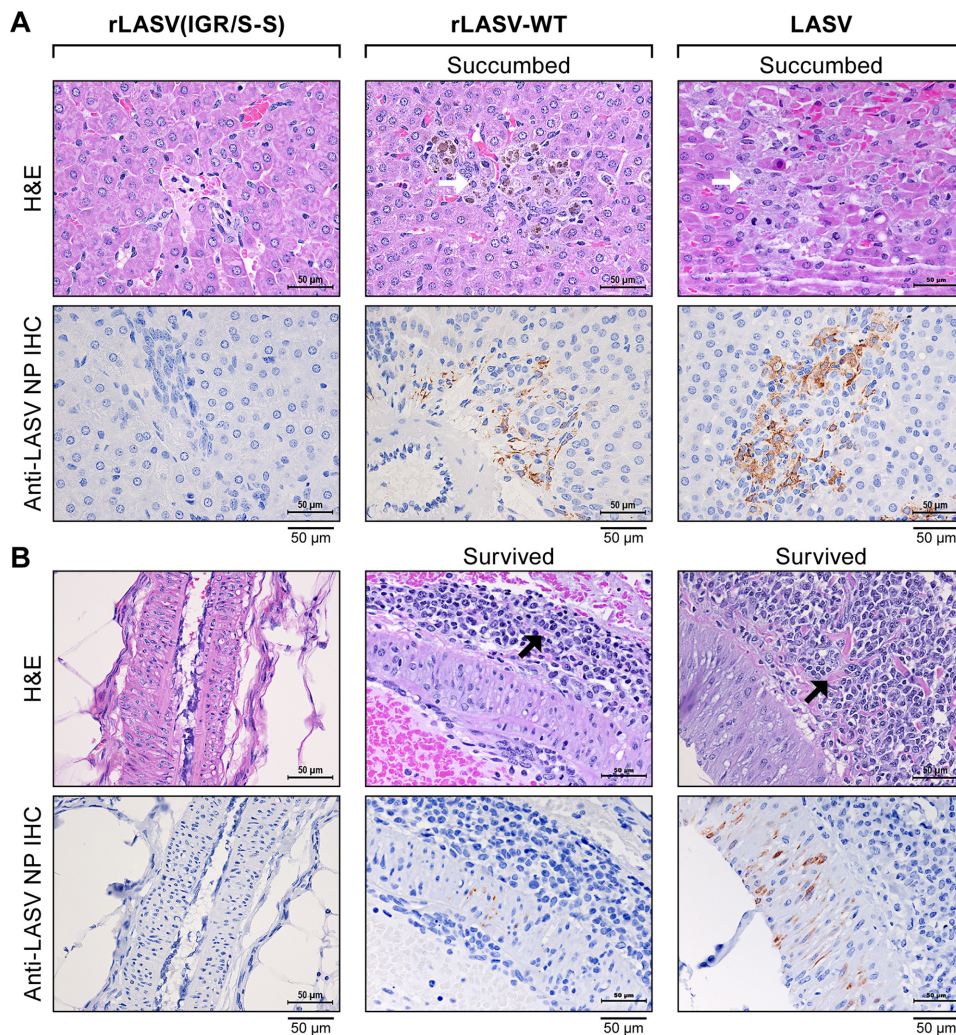
FIG 4 Histopathology and immunohistochemical staining of strain 13 guinea pigs inoculated with rLASV(IGR/S-S), rLASV-WT, or LASV. (A) Liver tissue section. White arrows indicate liver necrosis. (B) Kidney artery section. Black arrows indicate periarteritis. H&E staining or IHC staining with anti-LASV-NP MAb was performed as indicated at the left. Brown coloring indicates positive anti-LASV NP staining. Scale bars = 50 μm. H&E, hematoxylin and eosin; IHC, immunohistochemistry.

(9.32×10^3 vRNA copies/ml) were detected at day 7 p.e. from one rLASV(IGR/S-S)-inoculated guinea pig (Fig. 3E). In contrast, in rLASV-WT-exposed or LASV-exposed guinea pigs, high concentrations of vRNAs were detected in blood samples collected at day 7 and day 14 p.e. (average 10^5 to 10^6 LASV vRNA copies/ml) (Fig. 3E). As with the blood samples, vRNAs were not detected in tissues collected from rLASV(IGR/S-S)-inoculated guinea pigs at the experimental endpoint (Fig. 3F). In contrast, vRNAs were detected in most tissues tested from rLASV-WT-inoculated or LASV-inoculated animals (Fig. 3F). Anti-LASV IgG plasma titers determined by enzyme-linked immunosorbent assay (ELISA) (Fig. 3G) were detected in rLASV(IGR/S-S)-inoculated guinea pigs, suggesting that they were infected with rLASV(IGR/S-S). No anti-LASV neutralization antibody (nAb) titer was detected in the sera of rLASV(IGR/S-S)-inoculated guinea pigs at the study endpoint (data not shown).

Significant histopathological lesions were not observed in the examined tissues of rLASV(IGR/S-S)-inoculated guinea pigs (Fig. 4A), and all examined tissues from rLASV(IGR/S-S)-inoculated guinea pigs were negative for LASV antigen (Fig. 4). In contrast, typical acute LF lesions, including those resulting from interstitial pneumonia (data not shown), hepatic degeneration and necrosis (Fig. 4A, white arrow), endocar-

ditis (data not shown), and splenic lymphoid depletion (data not shown), were observed in all guinea pigs that succumbed to rLASV-WT or LASV infection. Positive LASV antigen staining was observed mainly in macrophages, epithelial cells, and/or arterial endothelial cells. Consistent with previous findings (38), mild to moderate systemic, lymphoplasmacytic, and histiocytic perivasculitis (Fig. 4B, black arrow) was observed in guinea pigs that survived rLASV-WT or LASV infection. Positive LASV antigen staining was noted in the smooth muscle cells in the tunicae mediae of large renal arteries (Fig. 4B). Overall, these results demonstrated the attenuation of rLASV(IGR/S-S) in strain 13 guinea pigs.

Protective efficacy of rLASV(IGR/S-S) against a typically lethal LASV exposure in strain 13 guinea pigs. To test whether a single dose of rLASV(IGR/S-S) could provide protection to strain 13 guinea pigs against a typically lethal LASV exposure, strain 13 guinea pigs were immunized with 10^5 PFU of rLASV(IGR/S-S) s.c. ($n = 4$) or with phosphate-buffered saline (PBS) as an immunization control ($n = 5$) (Fig. 5). At 30 days postimmunization (p.i.), these guinea pigs were exposed to 10^5 PFU of LASV s.c., and animals were monitored daily for clinical signs of infection throughout the study. Like the previous observation (Fig. 3), guinea pigs immunized with rLASV(IGR/S-S) did not develop any clinical signs of disease (Fig. S2A) or of abnormal weight loss (Fig. S2B), although transient elevated temperatures were observed from day 8 p.i. (day -22 p.e.) to day 13 p.i. (day -17 p.e.) (Fig. S2C). All rLASV(IGR/S-S)-immunized guinea pigs survived the typically lethal exposure to LASV (Fig. 5A) without developing any clinical signs of disease (Fig. 5B), weight loss (Fig. 5C), or elevated temperatures (Fig. 5D). In contrast, all mock-immunized guinea pigs developed classic disease signs of LASV infection (Fig. 5B), began losing weight at day 8 p.e. (Fig. 5C), and had elevated ($>40°C$) temperatures at day 9 p.e. (Fig. 5D). In the mock-immunization group, 3 of 5 guinea pigs succumbed to LASV infection on days 15 to 16 p.e., one guinea pig developed mild to moderate clinical signs until the study endpoint, and one guinea pig had mild clinical signs and recovered from infection (Fig. 5A and B).

On days -16 and -2 pre-LASV exposure [days 14 and 28 after rLASV(IGR/S-S) immunization], viremia was not detected by RT-qPCR in rLASV(IGR/S-S)-immunized animals (Fig. 5E). At day 12 after LASV exposure, viremia was detected in all mock-immunized animals (average 10^6 LASV vRNA copies/ml) but not in rLASV(IGR/S-S)-immunized animals (Fig. 5E). No vRNA was found in tissues tested from rLASV(IGR/S-S)-immunized animals (Fig. 5F). No significant histopathological lesions or tissue LASV antigen was observed in rLASV(IGR/S-S)-immunized guinea pigs (data not shown). Anti-LASV IgG serum titers were detected 2 weeks after immunization (day -16 pre-LASV exposure) with rLASV(IGR/S-S) and increased by week 4 after immunization (day -2 pre-LASV exposure). However, anti-LASV IgG antibody titers were not significantly boosted after LASV exposure (Fig. 5G). Anti-LASV neutralization titers were detected in the sera of rLASV(IGR/S-S)-immunized guinea pigs at the end of study [day 42 after LASV exposure, day 72 after rLASV(IGR/S-S) immunization] (Fig. 5H). Taken together, these data demonstrate that a single administration of rLASV(IGR/S-S) completely protected strain 13 guinea pigs from LASV infection and disease.

Attenuation and protective efficacy of rLASV(IGR/S-S) against a typically lethal GPA-LASV exposure in Hartley guinea pigs. Next, a low dose of rLASV(IGR/S-S) was evaluated for efficacy to protect against LASV infection. Hartley (outbred) guinea pigs are less sensitive than strain 13 (inbred) guinea pigs to LASV infection, with 30% lethality following s.c. administration of 2.4×10^4 PFU (37). However, intraperitoneal (i.p.) administration of 10^4 PFU of guinea pig-adapted LASV isolate Josiah (GPA-LASV) in Hartley guinea pigs results in $\geq80\%$ lethality (reference 39 and unpublished data). Given the limited availability of strain 13 guinea pigs, the Hartley model is attractive for testing the efficacy of LASV therapeutic and vaccine candidates (39, 40). We immunized three groups of Hartley guinea pigs s.c. with 10^2 PFU (low dose, $n = 8$) or 10^4 PFU (high dose, $n = 8$) of rLASV(IGR/S-S) or with PBS ($n = 7$). Hartley guinea pigs immunized with rLASV(IGR/S-S) did not develop any clinical signs of disease from immunization alone (Fig. 6A), including abnormal weight loss (Fig. 6B), although transient elevated tem-
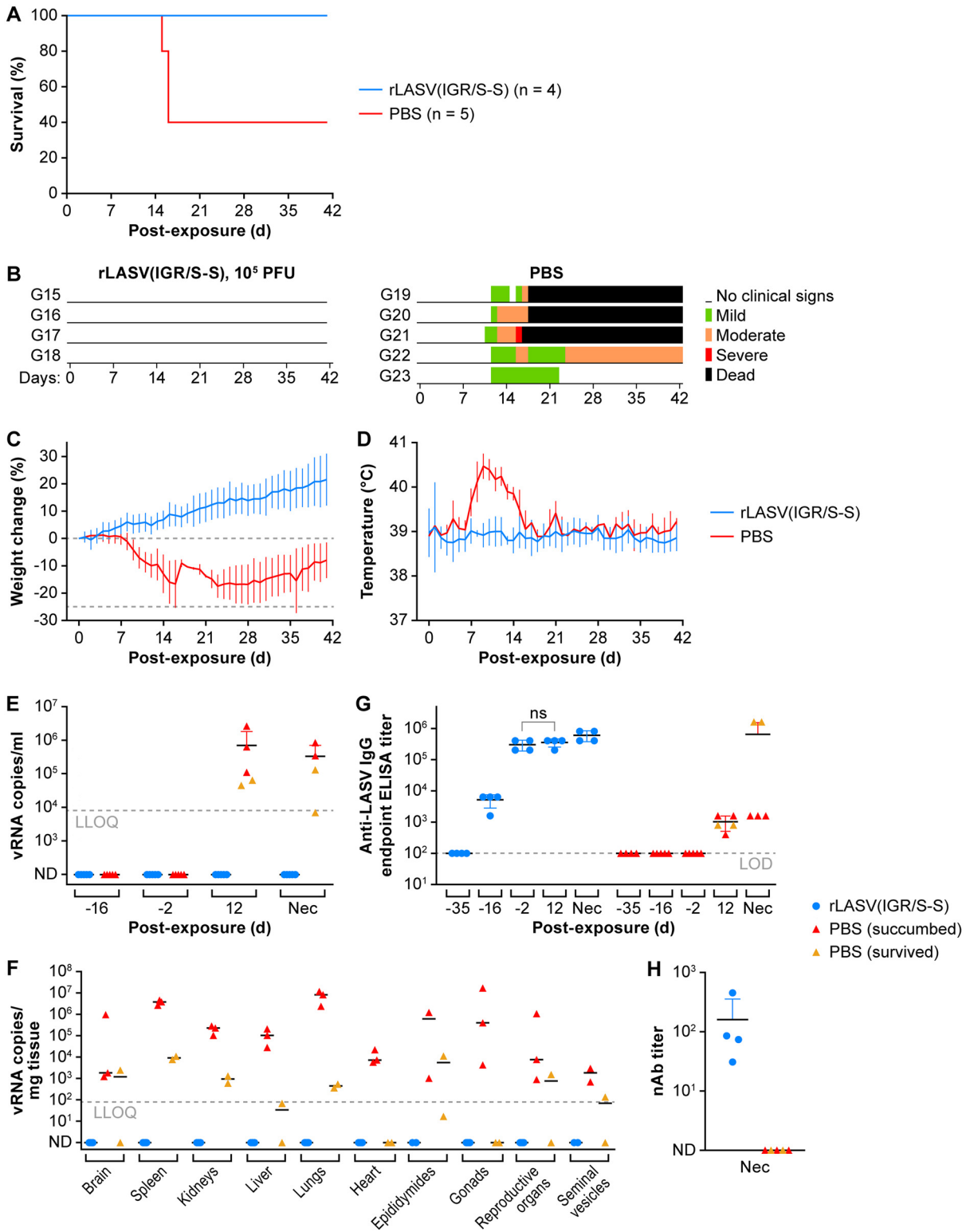
FIG 5 rLASV(IGR/S-S) provided protection against LASV infection in strain 13 guinea pigs. Strain 13 guinea pigs were immunized s.c. with 10^5 PFU of rLASV(IGR/S-S) ($n = 4$) or mock-immunized with PBS ($n = 5$). At day 30 p.i., guinea pigs were s.c. challenged with 10^5 PFU of LASV. (A to D) Survival (A), clinical scores (B), body weight loss (C), and temperature changes (D) were monitored daily for 42 days. (E and F) Viral loads in the blood at different times pre- and postexposure (E) and viral load in the indicated tissues at necropsy (F) were measured by RT-qPCR. (G) Anti-LASV IgG titers were determined by ELISA. ns, $P > 0.05$ (Student's t test). (H) Anti-LASV neutralizing antibody titers were measured. LLOQ, lower limit of quantification (panels E and F); LOD, limit of detection (panel G); ND, not detected; Nec, necropsy date; ns, $P > 0.05$.
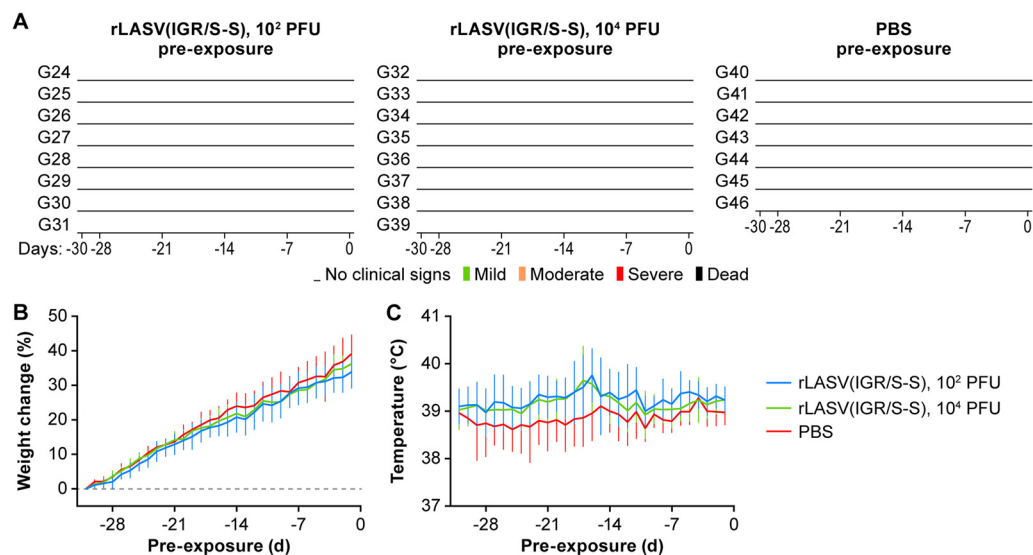
FIG 6 rLASV(IGR/S-S) is attenuated in Hartley guinea pigs. Hartley guinea pigs were s.c. immunized with 10^2 or 10^4 PFU of rLASV(IGR/S-S) ($n = 8$) or mock-immunized with PBS ($n = 7$). Clinical scores (A), body weight changes (B), and temperature changes (C) resulting from immunization alone were monitored daily for 30 days.

peratures were observed in several rLASV(IGR/S-S)-immunized animals (Fig. 6C). These data demonstrate the attenuation of rLASV(IGR/S-S) in Hartley guinea pigs.

At 30 days postimmunization (p.i.), all immunized guinea pigs were exposed to a typically lethal dose of GPA-LASV (10^4 PFU) i.p. and monitored daily for clinical signs of infection, including body weight and temperature changes, throughout the study. All guinea pigs immunized with either 10^2 or 10^4 PFU of rLASV(IGR/S-S) were protected against GPA-LASV-associated disease without having any clinical signs of disease [$P = 0.0442$ for both doses of rLASV(IGR/S-S)] (Fig. 7A to D). In contrast, all mock-immunized guinea pigs developed clinical signs of disease, became febrile (>40°C), and began losing weight at day 8 p.e. (Fig. 7B to D). Three of seven guinea pigs from the control group succumbed to GPA-LASV infection at 13 to 16 days p.e., whereas the other four animals recovered from infection.

Viremia was assessed by RT-qPCR on days −16 and −2 preexposure [days 14 and 28 after rLASV(IGR/S-S) immunization]. At day −16 preexposure (day 14 p.i.), vRNAs were detected in 3 of 8 and 2 of 8 animals that were immunized with 10^2 and 10^4 PFU of rLASV-IGR(S-S), respectively. At day −2 preexposure (day 28 p.i.), vRNAs were not detected in blood of any of the rLASV(IGR/S-S)-immunized animals (Fig. 7E). Importantly, at day 12 after GPA-LASV exposure, vRNAs were detected in all mock-immunized guinea pigs (average 10^7 vRNA copies/ml) but not in any rLASV(IGR/S-S)-immunized animals (Fig. 7E). Likewise, high vRNA loads were detected in most of the tissues collected from mock-immunized animals that had succumbed to GPA-LASV infection (Fig. 7F, red). vRNAs were also detected in different tissues collected from mock-immunized animals that had recovered from GPA-LASV infection (Fig. 7F, orange). However, vRNAs were not detected in most tissues from rLASV(IGR/S-S)-immunized guinea pigs. The exception was a very low concentration of vRNAs (9.3×10 vRNA copies/mg tissue, i.e., below the lower limit of quantification [<LLOQ]) that was detected in the spleen of one guinea pig that had been immunized with 10^2 PFU of rLASV(IGR/S-S) (Fig. 7F, blue and green). No significant histopathological lesions or positive LASV antigen staining was detected in the tissues from rLASV(IGR/S-S)-immunized guinea pigs (data not shown).

Anti-LASV IgG titers were detected in rLASV(IGR/S-S)-immunized guinea pigs 2 weeks p.i. (day −16 preexposure to GPA-LASV) and continued to increase after 4 weeks (day −2 preexposure to GPA-LASV). However, anti-LASV IgG antibody titers were not significantly boosted after GPA-LASV exposure (Fig. 7G). Anti-LASV neutraliz-
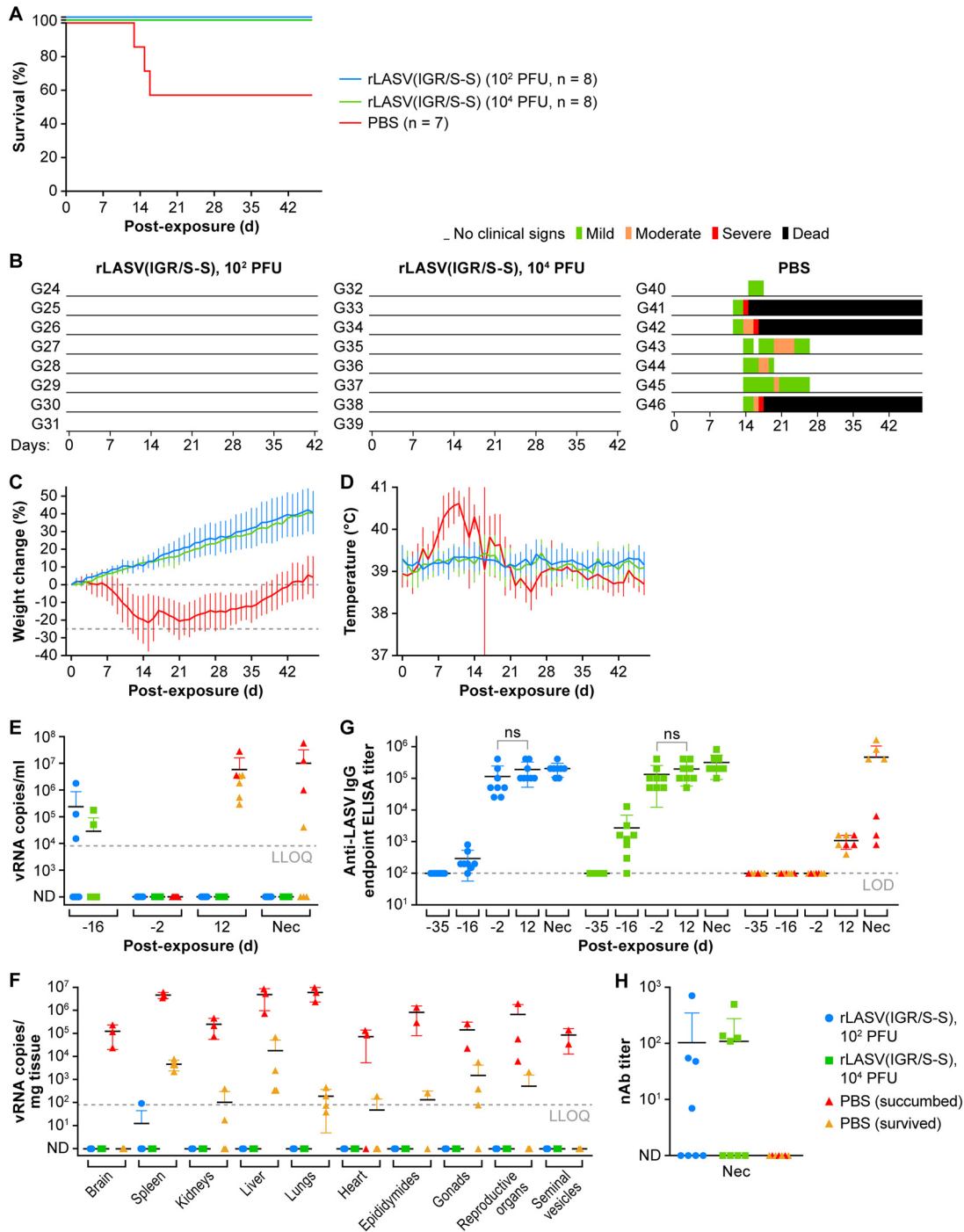
FIG 7 rLASV(IGR/S-S) provided protection against GPA-LASV infection in Hartley guinea pigs. rLASV(IGR/S-S)-immunized or mock-immunized Hartley guinea pigs from Fig. 6 were i.p. challenged with 10^4 PFU of GPA-LASV. (A to D) Survival (A), clinical scores (B), body weight changes (C), and temperature changes (D) were monitored daily for 47 days. (E and F) Viremia at different times pre- and postexposure (E) and viral load in the indicated tissues at necropsy (F) were measured by RT-qPCR. (G) Anti-LASV IgG titers were measured by ELISA. ns, $P > 0.05$ (Student's t test). (H) Anti-LASV nAb titers at necropsy were measured. LLOQ, lower limit of quantification (panels E and F); LOD, limit of detection (panel G); ND, not detected; Nec, necropsy date.

ing antibodies were detected in the serum of 8 of 16 guinea pigs immunized with rLASV(IGR/S-S) and exposed to GPA-LASV, suggesting that neutralization antibodies do not play an important role in the protection provided by rLASV(IGR/S-S) (Fig. 7H). Taken together, these data demonstrate that Hartley guinea pigs were completely protected from LASV infection after a single administration of a low rLASV(IGR/S-S) dose.
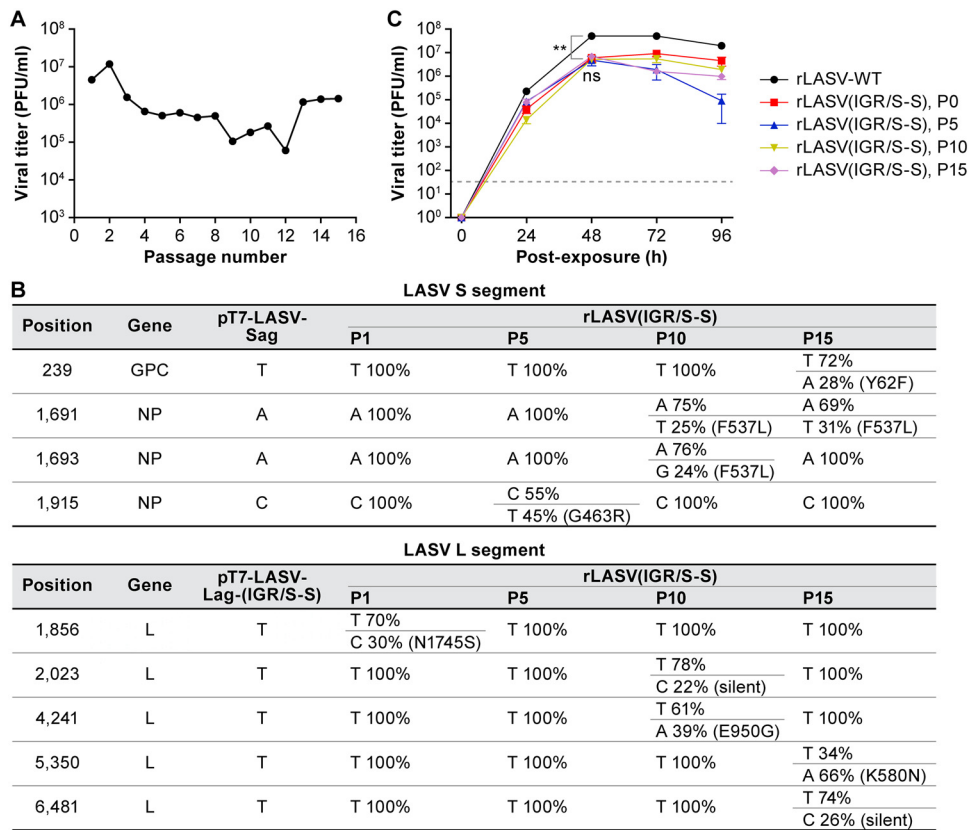
FIG 8 rLASV(IGR/S-S) is genetically stable during serial passages in cultured cells. (A) Viral titer of rLASV(IGR/S-S) at different passages. rLASV(IGR/S-S) was serially passaged in Vero cells at an MOI of 0.01. (B) Nucleotide and amino acid residue changes of rLASV(IGR/S-S) after serial passages in Vero cells. Viral RNAs from P1, P5, P10, and P15 of rLASV(IGR/S-S) were extracted and subjected to NGS analysis. (C) Growth kinetics of rLASV(IGR/S-S) in Vero cells (MOI = 0.01) at P0, P5, P10, and P15. At the indicated times p.e., TCS were harvested, and viral titers were measured by plaque assay. Data represent means ± SD of results from triplicate samples. **, $P < 0.01$; ns, $P > 0.05$ (Student's t test).

rLASV(IGR/S-S) is genetically stable during serial passages in cultured cells. To develop any LAV, evaluation of the genetic stability of LAV during multiplication in infected cells is critical. Therefore, the genetic stability of rLASV(IGR/S-S) *in vitro* was investigated by serial passaging in Vero cells. To that end, Vero cells were inoculated (MOI = 0.01) with rLASV(IGR/S-S) and at 72 h p.e., TCS were collected (passage 1 [P1]), and viral titers were determined by plaque assay. Fresh Vero cells were inoculated (MOI = 0.01) with rLASV(IGR/S-S) P1, and this process was serially repeated for a total of 15 passages (P15). Endpoint titers of each passage were in the range from 10^5 to 10^7 PFU/ml (Fig. 8A). The full-length viral genome sequences collected at P1, P5, P10, and P15 were analyzed by next-generation sequencing (NGS), and single nucleotide polymorphisms (SNPs) with frequencies greater than 20% were recorded (Fig. 8B). All SNPs detected within the S-IGR sequence in the L segment remained at a low level (2.33% ± 1.95) during serial passages in Vero cells. Several mutations occurred in the remainder of the L segment (e.g., T1856C, T2023C, and T4241A) and in the S segment (e.g., C1915T), which undulated in frequency during passages, suggesting that these mutations may not confer significant selective advantages. A single nucleotide polymorphism (SNP), A1691T, accumulated in the S segment during P10 to P15. At P15, SNPs T239A (Y62F) in the GPC gene of the S segment and T5350A (K580N) in the L gene were present at low frequency. To test the impact of these SNPs on viral fitness, the growth kinetics of rLASV(IGR/S-S) in Vero cells at an MOI of 0.01 were compared at P0, P5, P10, and P15. rLASV(IGR/S-S) from these passages had similar growth kinetics in Vero cells, and the viral peak titers were not statistically significantly different ($P > 0.05$),

suggesting that the mutations described above did not impact viral fitness in cell culture (Fig. 8C). These results demonstrate that rLASV(IGR/S-S) was genetically stable up to 15 passages in Vero cells.

DISCUSSION

Fifty years after its first description, LF still poses a major public health burden in the regions where it is endemic in Western Africa. The recent LF outbreaks in Nigeria (41, 42), together with the lack of licensed medical countermeasures to combat LASV infection, underscore the urgent need for LASV vaccine development (43). Epidemiological studies and nonhuman primate studies provided evidence supporting the concept that LASV-specific cell-mediated immune responses are associated with effective control of virus replication and subsequent recovery (44, 45). Although passive transfer of a cocktail of engineered human neutralization antibodies (nAbs) provided protective efficacy in LASV animal models (46–48), LASV nAbs appeared at low titers in convalescing patients several months after initial infection (49, 50). These discrepant results indicate that nAbs probably do not contribute to viral control and recovery from acute infection.

Following a single immunization, LAVs often induce long-term robust cell-mediated and humoral immune response (34) and represent the most feasible and attractive approach to combat LF within areas of endemicity. Several LF vaccine platforms based on recombinant viral vectors, including vaccinia virus (51, 52), vesicular stomatitis Indiana virus (VSIV) (53, 54), Mopeia virus (MOPV) (55), yellow fever virus (56, 57), measles virus (MeV) (58), and reassortant ML29 carrying the L segment from the nonpathogenic MOPV and the LASV S segment (59–62), have given promising results in LASV animal models, including nonhuman primates. Recombinant VSIV expressing LASV GPC (rVSV-LASV/GPC), recombinant MeV (rMeV)-expressing LASV GP and NP, chimpanzee adenovirus (ChAdOxl) expressing LASV-GPC, and mRNA-based or and DNA-based vaccine candidates represent five different LASV vaccine platforms currently funded by the Coalition for Epidemiological Preparedness Innovation (CEPI) to accelerate LASV vaccine development. Nevertheless, effective immunization with rVSV-LASV/GPC requires a high dose that might cause significant VSIV-associated side effects (63, 64), and rMV-LASV does not provide sterilizing immunity against LASV infection (58), which leaves room for exploring other vaccine platforms.

The mammarenavirus IGRs play critical roles in viral gene expression and infectious particle production (29). We previously demonstrated the feasibility of replacement of the L-IGR in the L segment with the S-IGR in LCMV, generating a recombinant rLCMV/IGR(S-S) (30). Although this rLCMV(IGR/S-S) grew to a relatively high titer in cultured cells *in vitro*, the virus was highly attenuated *in vivo* and provided complete protection to immunized laboratory mice against typically lethal LCMV-WT exposure (30). In the present study, we used the same attenuation strategy to generate rLASV(IGR/S-S), in which the L-IGR in the L segment was replaced with the S-IGR. Although rLASV(IGR/S-S) exhibited a moderate decrease in viral fitness in cultured cells compared to rLASV-WT, its viral titer still reached 1×10^6 PFU/ml in Vero cells. Such a high viral titer response is important to develop a cost-effective LAV vaccine. Moreover, rLASV(IGR/S-S) was highly attenuated in both strain 13 and Hartley guinea pigs. Importantly, immunization with only 10^2 PFU of rLASV(IGR/S-S) was able to protect these guinea pigs against an otherwise lethal exposure to LASV. Consistent with results from other LASV vaccine platform studies (34, 39, 58, 65), protection against an otherwise lethal dose of LASV in guinea pigs immunized with rLASV(IGR/S-S) occurred in the absence of detectable titers of LASV-specific neutralizing antibodies.

Genetic stability is a critical feature of an LAV candidate. A common concern about viral LAV is their potential for reversion to a more virulent phenotype, which is particularly important for RNA viruses because their error-prone replication machinery enables rapid evolution. On the basis of our findings with LCMV (30, 31), we expect that the underlying mechanism of attenuation of rLASV(IGR/S-S) involves altered control of virus gene expression caused by a well-defined genetic determinant, namely, the

replacement of the L-IGR by the S-IGR. This attenuated virus exhibited high genetic stability during serial passages in Vero cells, indicating that the emergence of rLASV(IGR/S-S) variants with increased virulence is unlikely.

Our previous findings obtained with LCMV (30, 31), together with those we report here for LASV, indicate that replacement of the L-IGR by the S-IGR could represent a general molecular strategy for mammarenavirus attenuation. This approach has the advantage that the corresponding recombinant virus retains the same antigenic composition and, therefore, immunogenicity potential as the parental pathogenic strain.

The development of LASV reverse genetics has provided us a novel powerful tool to manipulate the LASV genome. Combined with the safety features provided by the manipulation of IGRs with other attenuation strategies such as codon-deoptimization (CD) (66, 67), the generated LASV LAV could provide broad cross-protection against isolates from different LASV lineages while exhibiting optimal safety profiles.

MATERIALS AND METHODS

Cell lines. The sources and growing conditions of human adenocarcinoma alveolar basal epithelial A549, human embryonic kidney epithelial HEK293T/17, and grivet (*Chlorocebus aethiops*) kidney epithelial Vero cells and Vero E6 cells (BEI Resources, Manassas, VA, USA; catalog no. BR596) were previously described (65).

Viruses. All experiments associated with LASV were performed under conditions of maximum containment (biosafety level 4 [BSL-4]) at the Integrated Research Facility at Fort Detrick (IRF-Frederick) following approved standard operating procedures. LASV isolate Josiah and guinea pig-adapted LASV isolate Josiah (GPA-LASV) (68) were provided by the U.S. Army Medical Research Institute of Infectious Diseases (Fort Detrick, Frederick, MD, USA). LASV, GPA-LASV (stock IRF0205) (L segment, GenBank accession number KY425651.1; S segment, GenBank accession number KY425643.1) (39), recombinant Josiah isolate-based virus stocks [rLASV-WT, green-fluorescent protein-expressing rLASV (rLASV-GFP), and rLASV(IGR/S-S)] were grown and harvested and virus titers were determined as described previously (35).

Plasmids. pCAGGS expression plasmids encoding LASV-L (pCAGGS LASV-L), LASV-NP (pCAGGS LASV-NP), and T7 polymerase (pCAGGS T7) were described previously (35, 69). To generate plasmid pT7-LASV-Sag, able to direct T7 RNA polymerase (T7pol)-mediated synthesis of full-length LASV S genome RNA, mPol-I-LASV-Sag was digested with AvrII. The generated DNA fragment encoding the LASV 3′ untranslated region (3′-UTR), NP, IGR, GPC, and 5′-UTR was cloned into a T7pol-based LCMV S genome RNA-expressing plasmid [pT7-S(+)HR] (70). This plasmid was digested with AvrII to remove the LCMV S genome segment. Generation of plasmid pT7-LASV-Lag, able to direct T7pol-mediated synthesis of full-length LASV L genome, RNA was previously described (65). All restriction enzymes used in the construction of pT7-LASV-Lag were purchased from New England Biolabs (NEB; Ipswich, MA, USA). The L-IGR in pT7-LASV-Lag was replaced with the S-IGR to generate pT7-LASV-Lag-(IGR/S-S). Plasmid constructs were verified by DNA sequencing (ACGT Inc., Wheeling, IL, USA).

Rescue and propagation of rLASV(IGR/S-S). HEK293T/17 cells (7×10^5 cells/well, 6-well plate format) were cotransfected with pCAGGS LASV-NP (0.6 μg), pCAGGS LASV-L (1.0 μg), pCAGGS T7 (1.0 μg), pT7-LASV-Lag (rLASV-WT) (1.2 μg), pT7-LASV-Lag-(IGR/S-S) (1.2 μg), or [rLASV(IGR/S-S)], pT7-LASV-Sag (0.6 μg), using Lipofectamine 2000 (2.5 μl/μg DNA). At 5 h p.t., transfection mixture was replaced with Dulbecco's modified Eagle's medium (DMEM) containing 2% fetal bovine serum (FBS) (3 ml/well). Tissue culture supernatants (TCS) were collected at day 3 p.t. (P0D3) and day 6 p.t. (P0D6). At day 6 p.t., transfected HEK293T/T17 cells were cocultured with Vero cells, and TCS were collected 4 (P0D10 p.t.), 7 (P0D13 p.t.), and 11 (P0D17 p.t.) days after coculture. Virus titers were determined by plaque assay in Vero cells as described previously (35). rLASV-WT and LASV plaques were counted on day 4 postexposure (p.e.), and rLASV(IGR/S-S) plaques were counted on day 5 p.e. Image J software (NIH, Bethesda, MD, USA) was used to measure plaque size for 25 randomly selected plaques.

Virus growth kinetics comparison. A549 and Vero cells seeded in 24-well plates (2×10^5 cells/well) or 96-well plates (3×10^4 cells/well) were infected with rLASV(IGR/S-S) or rLASV-WT at an MOI of 0.01 or 0.1. Virus growth kinetics comparisons were performed as described previously (65).

Western blot analysis. A549 cells were inoculated with rLASV-WT or rLASV(IGR/S-S) (MOI = 0.1). At various times p.e., cell monolayers were lysed with cell lysis buffer (Cell Signaling Technology, Denver, MA, USA), and cell lysates were then subjected to gamma irradiation (50 kilosieverts [kSv]) before transferring them to the BSL-4 laboratory. Protein concentrations were measured using a bicinchoninic acid (BCA) protein assay kit (Pierce Biotechnology, Rockford, IL). Equivalent amounts (20 μg) of total cell lysates were resolved in 4% to 12% Bis-Tris NuPAGE gels (Thermo Fisher Scientific) and were then dry-transferred to nitrocellulose membranes (Thermo Fisher Scientific) by using an iBlot 2 gel transfer system (Thermo Fisher Scientific). Membranes were blocked with 5% nonfat milk–phosphate-buffered saline (PBS)–0.1% Tween (Sigma-Aldrich) for 1 h at room temperature. Membranes were incubated overnight with anti-LASV-GP2 polyclonal antibody, anti-LASV NP MAb, or anti-actin beta antibody as the loading control followed by incubation with horseradish peroxidase-conjugated secondary antibodies (Sigma-Aldrich) as described previously (65).

Animal studies. All animal studies were approved by the Division of Clinical Research Institutional Animal Care and Use Committee and performed at the IRF-Frederick, which is fully accredited by the Association for Assessment and Accreditation of Laboratory Animal Care International (AAALAC). Do-

mesticated guinea pigs (Rodentia: Caviidae: *Cavia porcellus* Linnaeus, 1758) were housed in an animal BSL-4 (ABSL-4) laboratory, monitored daily for signs of disease, including terminal signs, and humanely euthanized at terminal stages or at study endpoint (day 42 or day 47 p.e.), and necropsies were performed as previously described (65). To reduce the numbers of guinea pigs used, animal studies performed in the present work used the same control guinea pigs as those used as indicated in Fig. 3 to 6 of studies done previously to characterize an rLASV expressing a codon-deoptimized (CD) glyco-protein precursor (GPC) gene (rLASV-GPC/CD) (65).

Safety evaluation of rLASV(IGR/S-S) in strain 13 guinea pigs. Male and female strain 13 guinea pigs (6 to 16 weeks of age) obtained from the IRF-Frederick breeding colony were divided into three groups of 4 or 5 animals. Because of limited animal availability, the distributions into the groups were not proportional by age and sex. Guinea pigs were inoculated subcutaneously (s.c.) with 10^5 PFU of rLASV(IGR/S-S) ($n = 5$), rLASV-WT ($n = 4$), or LASV ($n = 5$). At days 7, 14, 21, 28, 35, and 42 p.e., blood samples from the cranial venae cavae were collected as described previously (65) to determine viral loads and Ab responses.

Evaluation of efficacy of rLASV(IGR/S-S) in strain13 guinea pigs. Strain 13 guinea pigs (aged 6 to 16 weeks) were immunized s.c. with 10^5 PFU of rLASV(IGR/S-S) ($n = 4$) or were mock-immunized with PBS ($n = 5$). At 30 days postimmunization (p.i.), all animals were injected s.c. with a typically lethal dose of LASV (10^5 PFU/animal), and blood samples were collected as previous described (65).

Efficacy evaluation of rLASV-IGR(S-S) in Hartley guinea pigs. Twenty-three Hartley guinea pigs (Charles River Laboratories, Wilmington, MA, USA) (aged 6 to 7 weeks; male and female) were divided into three groups, distributed proportionally by age and sex. Groups were immunized s.c. with 10^2 or 10^4 PFU of rLASV(IGR/S-S) ($n = 8$ per dose, $n = 16$ total) or were mock-immunized with PBS ($n = 7$). At 30 days p.i., all animals were injected intraperitoneally (i.p.) with 10^4 PFU of GPA-LASV. Blood samples were collected at day 5 before immunization, day 14 and 28 p.i., and day 12 p.e. to GPA-LASV.

Viral load measurement by RT-qPCR. Whole-blood and whole-tissue samples collected at necropsy were inactivated by the use of TRIzol LS (Thermo Fisher Scientific). Total RNA was isolated using a viral RNA minikit (Qiagen, Germantown, MD, USA). Briefly, 70 μl of TRIzol LS-inactivated sample was added to 280 μl of Buffer AVL (Qiagen) containing carrier RNA. After the binding and washing steps, the sample was eluted into 70 μl of Buffer AVE (Qiagen). Viral loads in the sample were measured using RT-qPCR as previously described (38, 71). The standard curve spanned 10^8 copies/reaction (upper limit of quantification [ULOQ]) through 10 copies/reaction (lower limit of quantification [LLOQ]). Transformed data from the whole-blood and whole-tissue samples were plotted in viral RNA copies ($\log_{10}$) per milliliter and viral RNA copies ($\log_{10}$) per milligram of tissue, respectively.

Endpoint anti-LASV IgG enzyme-linked immunosorbent assay. To measure LASV-specific anti-body titers, an IgG ELISA was developed in-house. The LASV antigens used in this assay were crude cell extracts generated from LASV-infected Vero cells. These extracts were lysed with radioimmunoprecipi-tation (RIPA) buffer (Cell Signaling Technology) and subjected to gamma irradiation (50 kSv) to inactivate viable virus before removal from the BSL-4 laboratory. Plates were coated with LASV-infected cell extracts diluted in coating buffer (Biolegend, San Diego, CA, USA) at a concentration of 50 ng/well, and the plates were stored at 4°C. The plates were washed six times with PBST (PBS plus 0.2% Tween 20 [Sigma-Aldrich]), and 300 μl of blocking buffer (PBST plus 3% normal chicken serum [Abcam] plus 2% milk [Thermo Fisher Scientific]) was added to each well. After incubation at 37°C for 2 h, heat-inactivated irradiated plasma that had been serially diluted 2-fold was added to the plates, and the plates were kept at 4°C overnight. After the plates were washed six times with PBST, goat anti-guinea pig IgG-horseradish peroxidase (Sigma-Aldrich) was added. The plates were incubated at 37°C for 1 h and washed again with PBST. Antibody-antigen complexes were revealed by adding 3,3',5,5'-tetramethylbenzidine substrate (Thermo Fisher Scientific) for 10 min at room temperature, and the reaction was stopped with stop solution. The absorbance was read at 450 nm on an Infinite M1000 plate reader (Tecan, Morrisville, NC, USA). The average signal from normal guinea pig plasma plus $3\times$ standard deviations was set as the cutoff value for endpoint titer measurement (72). Reciprocal serum dilutions corresponding to minimal binding were used to calculate titers.

Virus neutralization assays. Antibody neutralization titers were determined using a previously described fluorescence-based neutralization assay (35).

Histopathology and immunohistochemical staining. Tissue samples collected at necropsy were fixed in 10% NBF (formalin solution, neutral buffered) for at least 72 h before removal from the BSL-4 laboratory. Tissues were then embedded in paraffin, sectioned, mounted on glass slides, and stained with hematoxylin and eosin (H&E) following standard procedures. Immunohistochemistry (IHC) staining was performed with an anti-LASV-NP MAb (catalog no. 01-04-0104; Cambridge Biologics), followed by secondary and tertiary antibodies, and slides were examined and imaged as previously described (65).

Genetic stability assessment of rLASV(IGR/S-S) during serial passages in cell culture. To evaluate the genetic stability of rLASV(IGR/S-S) in cell culture, rLASV(IGR/S-S) was serially passaged 15 times in Vero cells. Briefly, Vero cells were infected with rLASV(IGR/S-S) in a 75-cm² flask (defined as passage 0 [P0]) at MOI = 0.01. At 72 h p.i., TCS (P1) were collected, and virus titer was measured by plaque assay. Then, fresh Vero cells were inoculated with P1 TCS (MOI = 0.01) to generate P2. This process was repeated to generate P15. P1, P5, P10, and P15 of rLASV(IGR/S-S) were inactivated and vRNA was extracted using a PureLink RNA minikit (Thermo Fisher Scientific). Each library from purified vRNA was prepared using SMARTer stranded total RNA-Seq kit v2—Pico input mammalian (TaKaRa Bio USA, Mountain View, CA, USA) according to the manufacturer's protocol and then sequenced on a HiSeq 3000 system (100-bp paired end). CLC Genomics Workbench 12 (Qiagen Digital Insights, Redwood City, CA,

USA) was used to align the NGS data with pT7-LASV-Lag-(IGR/S-S) and pT7-LASV-Sag plasmid sequence. The percentage of mutations was calculated based on the allele read counts.

Statistical analysis. Prism GraphPad 7 was used for all statistical analyses as previously described (65).

Data availability. All relevant data are available from the corresponding author upon request.

SUPPLEMENTAL MATERIAL

Supplemental material is available online only.

FIG S1, TIF file, 0.4 MB.

FIG S2, TIF file, 0.2 MB.

REFERENCES

1. Frame JD, Baldwin JM, Jr, Gocke DJ, Troup JM. 1970. Lassa fever, a new virus disease of man from West Africa. I. Clinical description and pathological findings. Am J Trop Med Hyg 19:670–676. https://doi.org/10.4269/ajtmh.1970.19.670.

2. Buckley SM, Casals J. 1970. Lassa fever, a new virus disease of man from West Africa. III. Isolation and characterization of the virus. Am J Trop Med Hyg 19:680–691. https://doi.org/10.4269/ajtmh.1970.19.680.

3. Monath TP, Newhouse VF, Kemp GE, Setzer HW, Cacciapuoti A. 1974. Lassa virus isolation from *Mastomys natalensis* rodents during an epidemic in Sierra Leone. Science 185:263–265. https://doi.org/10.1126/science.185.4147.263.

4. Fichet-Calvet E, Rogers DJ. 2009. Risk maps of Lassa fever in West Africa. PLoS Negl Trop Dis 3:e388. https://doi.org/10.1371/journal.pntd.0000388.

5. Gibb R, Moses LM, Redding DW, Jones KE. 2017. Understanding the cryptic nature of Lassa fever in West Africa. Pathog Glob Health 111:276–288. https://doi.org/10.1080/20477724.2017.1369643.

6. Buba MI, Dalhat MM, Nguku PM, Waziri N, Mohammad JO, Bomoi IM, Onyiah AP, Onwujei J, Balogun MS, Bashorun AT, Nsubuga P, Nasidi A. 2018. Mortality among confirmed Lassa fever cases during the 2015–2016 outbreak in Nigeria. Am J Public Health 108:262–264. https://doi.org/10.2105/AJPH.2017.304186.

7. Roberts L. 2018. Nigeria hit by unprecedented Lassa fever outbreak. Science 359:1201–1202. https://doi.org/10.1126/science.359.6381.1201.

8. Anonymous. 2018. Lassa fever and global health security. Lancet Infect Dis 18:357. https://doi.org/10.1016/S1473-3099(18)30179-8.

9. Kofman A, Choi MJ, Rollin PE. 2019. Lassa fever in travelers from West Africa, 1969–2016. Emerg Infect Dis 25:245–248. https://doi.org/10.3201/eid2502.180836.

10. Bausch DG, Hadi CM, Khan SH, Lertora JJ. 2010. Review of the literature and proposed guidelines for the use of oral ribavirin as postexposure prophylaxis for Lassa fever. Clin Infect Dis 51:1435–1441. https://doi.org/10.1086/657315.

11. Eberhardt KA, Mischlinger J, Jordan S, Groger M, Günther S, Ramharter M. 2019. Ribavirin for the treatment of Lassa fever: a systematic review and meta-analysis. Int J Infect Dis 87:15–20. https://doi.org/10.1016/j.ijid.2019.07.015.

12. World Health Organization. 2018. A research and development Blueprint for action to prevent epidemics. https://www.who.int/blueprint/en/.

13. Radoshitzky SR, Buchmeier MJ, Charrel RN, Clegg JCS, Gonzalez JJ, Gunther S, Hepojoki J, Kuhn JH, Lukashevich IS, Romanowski V, Salvato MS, Sironi M, Stenglein MD, de la Torre JC; ICTV Report Consortium. 2019. ICTV virus taxonomy profile: *Arenaviridae*. J Gen Virol 100:1200–1201. https://doi.org/10.1099/jgv.0.001280.

14. Lukashevich IS, Stelmakh TA, Golubev VP, Stchesljenok EP, Lemeshko NN. 1984. Ribonucleic acids of Machupo and Lassa viruses. Arch Virol 79:189–203. https://doi.org/10.1007/bf01310811.

15. Djavani M, Lukashevich IS, Sanchez A, Nichol ST, Salvato MS. 1997. Completion of the Lassa fever virus sequence and identification of a RING finger open reading frame at the L RNA 5' end. Virology 235:414–418. https://doi.org/10.1006/viro.1997.8722.

16. Lukashevich IS, Djavani M, Shapiro K, Sanchez A, Ravkov E, Nichol ST, Salvato MS. 1997. The Lassa fever virus L gene: nucleotide sequence, comparison, and precipitation of a predicted 250 kDa protein with monospecific antiserum. J Gen Virol 78:547–551. https://doi.org/10.1099/0022-1317-78-3-547.

17. Perez M, Craven RC, de la Torre JC. 2003. The small RING finger protein Z drives arenavirus budding: implications for antiviral strategies. Proc Natl Acad Sci U S A 100:12978–12983. https://doi.org/10.1073/pnas.2133782100.

18. Strecker T, Eichler R, Meulen J, Weissenhorn W, Dieter Klenk H-D, Garten W, Lenz O. 2003. Lassa virus Z protein is a matrix protein and sufficient for the release of virus-like particles [corrected]. J Virol 77:10700–10705. https://doi.org/10.1128/jvi.77.19.10700-10705.2003.

19. Auperin DD, Sasso DR, McCormick JB. 1986. Nucleotide sequence of the glycoprotein gene and intergenic region of the Lassa virus S genome RNA. Virology 154:155–167. https://doi.org/10.1016/0042-6822(86)90438-1.

20. Clegg JCS, Wilson SM, Oram JD. 1991. Nucleotide sequence of the S RNA of Lassa virus (Nigerian strain) and comparative analysis of arenavirus gene products. Virus Res 18:151–164. https://doi.org/10.1016/0168-1702(91)90015-N.

21. Hass M, Gölnitz U, Müller S, Becker-Ziaja B, Günther S. 2004. Replicon

system for Lassa virus. J Virol 78:13793–13803. https://doi.org/10.1128/JVI.78.24.13793-13803.2004.

22. Ortiz-Riaño E, Cheng BY, de la Torre JC, Martínez-Sobrido L. 2011. The C-terminal region of lymphocytic choriomeningitis virus nucleoprotein contains distinct and segregable functional domains involved in NP-Z interaction and counteraction of the type I interferon response. J Virol 85:13038–13048. https://doi.org/10.1128/JVI.05834-11.

23. Martínez-Sobrido L, Zúñiga EI, Rosario D, García-Sastre A, de la Torre JC. 2006. Inhibition of the type I interferon response by the nucleoprotein of the prototypic arenavirus lymphocytic choriomeningitis virus. J Virol 80:9192–9199. https://doi.org/10.1128/JVI.00555-06.

24. Rodrigo WW, Ortiz-Riaño E, Pythoud C, Kunz S, de la Torre JC, Martínez-Sobrido L. 2012. Arenavirus nucleoproteins prevent activation of nuclear factor kappa B. J Virol 86:8185–8197. https://doi.org/10.1128/JVI.07240-11.

25. Hastie KM, Kimberlin CR, Zandonatti MA, MacRae IJ, Saphire EO. 2011. Structure of the Lassa virus nucleoprotein reveals a dsRNA-specific 3′ to 5′ exonuclease activity essential for immune suppression. Proc Natl Acad Sci U S A 108:2396–2401. https://doi.org/10.1073/pnas.1016404108.

26. Lenz O, ter Meulen J, Klenk HD, Seidah NG, Garten W. 2001. The Lassa virus glycoprotein precursor GP-C is proteolytically processed by subtilase SKI-1/S1P. Proc Natl Acad Sci U S A 98:12701–12705. https://doi.org/10.1073/pnas.221447598.

27. Jae LT, Raaben M, Herbert AS, Kuehne AI, Wirchnianski AS, Soh TK, Stubbs SH, Janssen H, Damme M, Saftig P, Whelan SP, Dye JM, Brummelkamp TR. 2014. Lassa virus entry requires a trigger-induced receptor switch. Science 344:1506–1510. https://doi.org/10.1126/science.1252480.

28. Cohen-Dvashi H, Cohen N, Israeli H, Diskin R. 2015. Molecular mechanism for LAMP1 recognition by Lassa virus. J Virol 89:7584–7592. https://doi.org/10.1128/JVI.00651-15.

29. Pinschewer DD, Perez M, de la Torre JC. 2005. Dual role of the lymphocytic choriomeningitis virus intergenic region in transcription termination and virus propagation. J Virol 79:4519–4526. https://doi.org/10.1128/JVI.79.7.4519-4526.2005.

30. Iwasaki M, Ngo N, Cubitt B, Teijaro JR, de la Torre JC. 2015. General molecular strategy for development of arenavirus live-attenuated vaccines. J Virol 89:12166–12177. https://doi.org/10.1128/JVI.02075-15.

31. Iwasaki M, Cubitt B, Sullivan BM, de la Torre JC. 2016. The high degree of sequence plasticity of the arenavirus noncoding intergenic region (IGR) enables the use of a nonviral universal synthetic IGR To attenuate arenaviruses. J Virol 90:3187–3197. https://doi.org/10.1128/JVI.03145-15.

32. Bergeron E, Chakrabarti AK, Bird BH, Dodd KA, McMullan LK, Spiropoulou CF, Nichol ST, Albariño CG. 2012. Reverse genetics recovery of Lujo virus and role of virus RNA secondary structures in efficient virus growth. J Virol 86:10759–10765. https://doi.org/10.1128/JVI.01144-12.

33. Golden JW, Beitzel B, Ladner JT, Mucker EM, Kwilas SA, Palacios G, Hooper JW. 2017. An attenuated Machupo virus with a disrupted L-segment intergenic region protects guinea pigs against lethal Guanarito virus infection. Sci Rep 7:4679. https://doi.org/10.1038/s41598-017-04889-x.

34. Falzarano D, Feldmann H. 2013. Vaccines for viral hemorrhagic fevers–progress and shortcomings. Curr Opin Virol 3:343–351. https://doi.org/10.1016/j.coviro.2013.04.007.

35. Caì Y, Iwasaki M, Beitzel BF, Yú S, Postnikova EN, Cubitt B, DeWald LE, Radoshitzky SR, Bollinger L, Jahrling PB, Palacios GF, de la Torre JC, Kuhn JH. 2018. Recombinant Lassa virus expressing green fluorescent protein as a tool for high-throughput drug screens and neutralizing antibody assays. Viruses 10:E655. https://doi.org/10.3390/v10110655.

36. Yun NE, Seregin AV, Walker DH, Popov VL, Walker AG, Smith JN, Miller M, de la Torre JC, Smith JK, Borisevich V, Fair JN, Wauquier N, Grant DS, Bockarie M, Bente D, Paessler S. 2013. Mice lacking functional STAT1 are highly susceptible to lethal infection with Lassa virus. J Virol 87:10908–10911. https://doi.org/10.1128/JVI.01433-13.

37. Jahrling PB, Smith S, Hesse RA, Rhoderick JB. 1982. Pathogenesis of Lassa virus infection in guinea pigs. Infect Immun 37:771–778. https://doi.org/10.1128/IAI.37.2.771-778.1982.

38. Liu DX, Perry DL, DeWald LE, Cai Y, Hagen KR, Cooper TK, Huzella LM, Hart R, Bonilla A, Bernbaum JG, Janosko KB, Adams R, Johnson RF, Kuhn JH, Schnell MJ, Crozier I, Jahrling PB, de la Torre JC. 2019. Persistence of Lassa virus associated with severe systemic arteritis in convalescing Guinea pigs (Cavia porcellus). J Infect Dis 219:1818–1822. https://doi.org/10.1093/infdis/jiy641.

39. Abreu-Mota T, Hagen KR, Cooper K, Jahrling PB, Tan G, Wirblich C, Johnson RF, Schnell MJ. 2018. Non-neutralizing antibodies elicited by recombinant Lassa-rabies vaccine are critical for protection against Lassa fever. Nat Commun 9:4223. https://doi.org/10.1038/s41467-018-06741-w.

40. Safronetz D, Rosenke K, Westover JB, Martellaro C, Okumura A, Furuta Y, Geisbert J, Saturday G, Komeno T, Geisbert TW, Feldmann H, Gowen BB. 2015. The broad-spectrum antiviral favipiravir protects guinea pigs from lethal Lassa virus infection post-disease onset. Sci Rep 5:14775. https://doi.org/10.1038/srep14775.

41. Adepoju P. 2019. Nigeria's unending war with Lassa fever. Lancet 393:627–628. https://doi.org/10.1016/S0140-6736(19)30357-5.

42. Siddle KJ, Eromon P, Barnes KG, Mehta S, Oguzie JU, Odia I, Schaffner SF, Winnicki SM, Shah RR, Qu J, Wohl S, Brehio P, Iruolagbe C, Aiyepada J, Uyigue E, Akhilomen P, Okonofua G, Ye S, Kayode T, Ajogbasile F, Uwanibe J, Gaye A, Momoh M, Chak B, Kotliar D, Carter A, Gladden-Young A, Freije CA, Omoregie O, Osiemi B, Muoebonam EB, Airende M, Enigbe R, Ebo B, Nosamiefan I, Oluniyi P, Nekoui M, Ogbaini-Emovon E, Garry RF, Andersen KG, Park DJ, Yozwiak NL, Akpede G, Ihekweazu C, Tomori O, Okogbenin S, Folarin OA, Okokhere PO, MacInnis BL, Sabeti PC, Happi CT. 2018. Genomic analysis of Lassa virus during an Increase in cases in Nigeria in 2018. N Engl J Med 379:1745–1753. https://doi.org/10.1056/NEJMoa1804498.

43. Salami K, Gouglas D, Schmaljohn C, Saville M, Tornieporth N. 2019. A review of Lassa fever vaccine candidates. Curr Opin Virol 37:105–111. https://doi.org/10.1016/j.coviro.2019.07.006.

44. Baize S, Marianneau P, Loth P, Reynard S, Journeaux A, Chevallier M, Tordo N, Deubel V, Contamin H. 2009. Early and strong immune responses are associated with control of viral replication and recovery in Lassa virus-infected cynomolgus monkeys. J Virol 83:5890–5903. https://doi.org/10.1128/JVI.01948-08.

45. Fisher-Hoch SP, Hutwagner L, Brown B, McCormick JB. 2000. Effective vaccine for Lassa fever. J Virol 74:6777–6783. https://doi.org/10.1128/jvi.74.15.6777-6783.2000.

46. Robinson JE, Hastie KM, Cross RW, Yenni RE, Elliott DH, Rouelle JA, Kannadka CB, Smira AA, Garry CE, Bradley BT, Yu H, Shaffer JG, Boisen ML, Hartnett JN, Zandonatti MA, Rowland MM, Heinrich ML, Martínez-Sobrido L, Cheng B, de la Torre JC, Andersen KG, Goba A, Momoh M, Fullah M, Gbakie M, Kanneh L, Koroma VJ, Fonnie R, Jalloh SC, Kargbo B, Vandi MA, Gbetuwa M, Ikponmwosa O, Asogun DA, Okokhere PO, Follarin OA, Schieffelin JS, Pitts KR, Geisbert JB, Kulakoski PC, Wilson RB, Happi CT, Sabeti PC, Gevao SM, Khan SH, Grant DS, Geisbert TW, Saphire EO, Branco LM, Garry RF. 2016. Most neutralizing human monoclonal antibodies target novel epitopes requiring both Lassa virus glycoprotein subunits. Nat Commun 7:11544. https://doi.org/10.1038/ncomms11544.

47. Cross RW, Mire CE, Branco LM, Geisbert JB, Rowland MM, Heinrich ML, Goba A, Momoh M, Grant DS, Fullah M, Khan SH, Robinson JE, Geisbert TW, Garry RF. 2016. Treatment of Lassa virus infection in outbred guinea pigs with first-in-class human monoclonal antibodies. Antiviral Res 133:218–222. https://doi.org/10.1016/j.antiviral.2016.08.012.

48. Mire CE, Cross RW, Geisbert JB, Borisevich V, Agans KN, Deer DJ, Heinrich ML, Rowland MM, Goba A, Momoh M, Boisen ML, Grant DS, Fullah M, Khan SH, Fenton KA, Robinson JE, Branco LM, Garry RF, Geisbert TW. 2017. Human-monoclonal-antibody therapy protects nonhuman primates against advanced Lassa fever. Nat Med 23:1146–1149. https://doi.org/10.1038/nm.4396.

49. Zapata JC, Medina-Moreno S, Guzmán-Cardozo C, Salvato MS. 2018. Improving the breadth of the host's immune response to Lassa virus. Pathogens 7:E84. https://doi.org/10.3390/pathogens7040084.

50. Russier M, Pannetier D, Baize S. 2012. Immune responses and Lassa virus infection. Viruses 4:2766–2785. https://doi.org/10.3390/v4112766.

51. Fisher-Hoch SP, McCormick JB, Auperin D, Brown BG, Castor M, Perez G, Ruo S, Conaty A, Brammer L, Bauer S. 1989. Protection of rhesus monkeys from fatal Lassa fever by vaccination with a recombinant vaccinia virus containing the Lassa virus glycoprotein gene. Proc Natl Acad Sci U S A 86:317–321. https://doi.org/10.1073/pnas.86.1.317.

52. Salvato MS, Domi A, Guzman-Cardozo C, Medina-Moreno S, Zapata JC, Hsu H, McCurley N, Basu R, Hauser M, Hellerstein M, Guirakhoo F. 2019. A single dose of modified vaccinia Ankara expressing Lassa virus-like particles protects mice from lethal intra-cerebral virus challenge. Pathogens 8:E133. https://doi.org/10.3390/pathogens8030133.

53. Geisbert TW, Jones S, Fritz EA, Shurtleff AC, Geisbert JB, Liebscher R, Grolla A, Ströher U, Fernando L, Daddario KM, Guttieri MC, Mothé BR, Larsen T, Hensley LE, Jahrling PB, Feldmann H. 2005. Development of a new vaccine for the prevention of Lassa fever. PLoS Med 2:e183. https://doi.org/10.1371/journal.pmed.0020183.

54. Safronetz D, Mire C, Rosenke K, Feldmann F, Haddock E, Geisbert T,

Feldmann H. 2015. A recombinant vesicular stomatitis virus-based Lassa fever vaccine protects guinea pigs and macaques against challenge with geographically and genetically distinct Lassa viruses. PLoS Negl Trop Dis 9:e0003736. https://doi.org/10.1371/journal.pntd.0003736.

55. Carnec X, Mateo M, Page A, Reynard S, Hortion J, Picard C, Yekwa E, Barrot L, Barron S, Vallve A, Raoul H, Carbonnelle C, Ferron F, Baize S. 2018. A vaccine platform against arenaviruses based on a recombinant hyperattenuated Mopeia virus expressing heterologous glycoproteins. J Virol 92:e02230-17. https://doi.org/10.1128/JVI.02230-17.

56. Bredenbeek PJ, Molenkamp R, Spaan WJM, Deubel V, Marianneau P, Salvato MS, Moshkoff D, Zapata J, Tikhonov I, Patterson J, Carrion R, Ticer A, Brasky K, Lukashevich IS. 2006. A recombinant yellow fever 17D vaccine expressing Lassa virus glycoproteins. Virology 345:299–304. https://doi.org/10.1016/j.virol.2005.12.001.

57. Jiang X, Dalebout TJ, Bredenbeek PJ, Carrion R, Jr, Brasky K, Patterson J, Goicochea M, Bryant J, Salvato MS, Lukashevich IS. 2011. Yellow fever 17D-vectored vaccines expressing Lassa virus GP1 and GP2 glycoproteins provide protection against fatal disease in guinea pigs. Vaccine 29:1248–1257. https://doi.org/10.1016/j.vaccine.2010.11.079.

58. Mateo M, Reynard S, Carnec X, Journeaux A, Baillet N, Schaeffer J, Picard C, Legras-Lachuer C, Allan R, Perthame E, Hillion K-H, Pietrosemoli N, Dillies M-A, Barrot L, Vallve A, Barron S, Fellmann L, Gaillard J-C, Armengaud J, Carbonnelle C, Raoul H, Tangy F, Baize S. 2019. Vaccines inducing immunity to Lassa virus glycoprotein and nucleoprotein protect macaques after a single shot. Sci Transl Med 11:eaaw3163. https://doi.org/10.1126/scitranslmed.aaw3163.

59. Lukashevich IS, Patterson J, Carrion R, Moshkoff D, Ticer A, Zapata J, Brasky K, Geiger R, Hubbard GB, Bryant J, Salvato MS. 2005. A live attenuated vaccine for Lassa fever made by reassortment of Lassa and Mopeia viruses. J Virol 79:13934–13942. https://doi.org/10.1128/JVI.79.22.13934-13942.2005.

60. Carrion R, Jr, Patterson JL, Johnson C, Gonzales M, Moreira CR, Ticer A, Brasky K, Hubbard GB, Moshkoff D, Zapata J, Salvato MS, Lukashevich IS. 2007. A ML29 reassortant virus protects guinea pigs against a distantly related Nigerian strain of Lassa virus and can provide sterilizing immunity. Vaccine 25:4093–4102. https://doi.org/10.1016/j.vaccine.2007.02.038.

61. Lukashevich IS, Carrion R, Jr, Salvato MS, Mansfield K, Brasky K, Zapata J, Cairo C, Goicochea M, Hoosien GE, Ticer A, Bryant J, Davis H, Hammamieh R, Mayda M, Jett M, Patterson J. 2008. Safety, immunogenicity, and efficacy of the ML29 reassortant vaccine for Lassa fever in small non-human primates. Vaccine 26:5246–5254. https://doi.org/10.1016/j.vaccine.2008.07.057.

62. Zapata JC, Poonia B, Bryant J, Davis H, Ateh E, George L, Crasta O, Zhang Y, Slezak T, Jaing C, Pauza CD, Goicochea M, Moshkoff D, Lukashevich IS, Salvato MS. 2013. An attenuated Lassa vaccine in SIV-infected rhesus macaques does not persist or cause arenavirus disease but does elicit Lassa virus-specific immunity. Virol J 10:52. https://doi.org/10.1186/1743-422X-10-52.

63. Huttner A, Dayer J-A, Yerly S, Combescure C, Auderset F, Desmeules J, Eickmann M, Finckh A, Goncalves AR, Hooper JW, Kaya G, Krähling V, Kwilas S, Lemaître B, Matthey A, Silvera P, Becker S, Fast PE, Moorthy V, Kieny MP, Kaiser L, Siegrist C-A; VSV-Ebola Consortium. 2015. The effect of dose on the safety and immunogenicity of the VSV Ebola candidate vaccine: a randomised double-blind, placebo-controlled phase 1/2 trial. Lancet Infect Dis 15:1156–1166. https://doi.org/10.1016/S1473-3099(15)00154-1.

64. Henao-Restrepo AM, Camacho A, Longini IM, Watson CH, Edmunds WJ, Egger M, Carroll MW, Dean NE, Diatta I, Doumbia M, Draguez B, Duraffour S, Enwere G, Grais R, Gunther S, Gsell P-S, Hossmann S, Watle SV, Kondé MK, Kéïta S, Kone S, Kuisma E, Levine MM, Mandal S, Mauget T, Norheim G, Riveros X, Soumah A, Trelle S, Vicari AS, Røttingen J-A, Kieny M-P. 2017. Efficacy and effectiveness of an rVSV-vectored vaccine in preventing Ebola virus disease: final results from the Guinea ring vaccination, open-label, cluster-randomised trial (Ebola Ça Suffit!). Lancet 389:505–518. https://doi.org/10.1016/S0140-6736(16)32621-6.

65. Cai Y, Ye C, Cheng B, Nogales A, Iwasaki M, Yu S, Cooper K, Liu DX, Hart R, Adams R, Brady T, Postnikova EN, Kurtz J, St Claire M, Kuhn JH, de la Torre JC, Martínez-Sobrido L. 2020. A Lassa fever live attenuated vaccine based on codon deoptimization of the viral glycoprotein gene. mBio 11:e00039-20. https://doi.org/10.1128/mBio.00039-20.

66. Cheng BY, Ortiz-Riaño E, Nogales A, de la Torre JC, Martínez-Sobrido L. 2015. Development of live-attenuated arenavirus vaccines based on codon deoptimization. J Virol 89:3523–3533. https://doi.org/10.1128/JVI.03401-14.

67. Cheng BYH, Nogales A, de la Torre JC, Martínez-Sobrido L. 2017. Development of live-attenuated arenavirus vaccines based on codon deoptimization of the viral glycoprotein. Virology 501:35–46. https://doi.org/10.1016/j.virol.2016.11.001.

68. Cashman KA, Wilkinson ER, Wollen SE, Shamblin JD, Zelko JM, Bearss JJ, Zeng X, Broderick KE, Schmaljohn CS. 2017. DNA vaccines elicit durable protective immunity against individual or simultaneous infections with Lassa and Ebola viruses in guinea pigs. Hum Vaccin Immunother 13:3010–3019. https://doi.org/10.1080/21645515.2017.1382780.

69. Martínez-Sobrido L, Cheng BY, de la Torre JC. 2016. Reverse genetics approaches to control arenavirus. Methods Mol Biol 1403:313–351. https://doi.org/10.1007/978-1-4939-3387-7_17.

70. Sánchez AB, de la Torre JC. 2006. Rescue of the prototypic arenavirus LCMV entirely from plasmid. Virology 350:370–380. https://doi.org/10.1016/j.virol.2006.01.012.

71. Nikisins S, Rieger T, Patel P, Müller R, Günther S, Niedrig M. 2015. International external quality assessment study for molecular detection of Lassa virus. PLoS Negl Trop Dis 9:e0003793. https://doi.org/10.1371/journal.pntd.0003793.

72. Frey A, Di Canzio J, Zurakowski D. 1998. A statistically defined endpoint titer determination method for immunoassays. J Immunol Methods 221:35–41. https://doi.org/10.1016/s0022-1759(98)00170-7.